Vapor-phase tertiary butylation of phenol over mesoporous gallosilicate molecular sieves †

Ayyamperumal Sakthivel and Parasuraman Selvam *

Department of Chemistry, Indian Institute of Technology-Bombay, Powai, Mumbai 400 076, India

Received 24 May 2002; accepted 17 July 2002

Isomorphously substituted GaMCM-41 molecular sieves with different Si : Ga ratio were synthesized and characterized systematically by various analytical and spectroscopic techniques. Temperature-programmed desorption of ammonia was used to identify the nature of acidic sites. For the first time, the vapor-phase tertiary butylation of phenol reaction was carried out over protonated GaMCM-41. The catalysts showed higher (phenol) conversion and good (*para-tertiary* butyl phenol) selectivity over the Al- and Fe-analogs of MCM-41. Further, the gallosilicates showed good stability both before and after the reaction compared to the aluminosilicates or ferrisilicates.

KEY WORDS: H-GaMCM-41; *tertiary* butylation; acid catalysts; *para-tertiary* butyl phenol.

1. Introduction

Alkyl phenols are of great commercial importance, as their derivatives have a variety of applications ranging from surfactants to pharmaceuticals [1,2]. In particular, one of the tertiary butylated products of phenol, viz. *para-tertiary*-butyl phenol (*p-t*-BP), is consumed (~60–70%) in phenolic resin synthesis [2]. Furthermore, it is also used as antioxidants, synthetic lubricants and ingredients in demulsifiers and polymer inhibitors, as well as in the production of triaryl phosphates. In general, the tertiary butylation of phenol reaction is carried out using environmentally hazardous sulfuric acid, fluoro sulfonic acid, phosphoric acid and aluminum chloride-boric acid catalysts and isobutylene as the alkylating agent [1–3]. However, owing to numerous problems associated with the use of homogeneous catalysts, considerable attention has been focused on the development of solid acid (heterogeneous) catalysts, *e.g.*, cation exchange resins, pillared clays, sulfated zirconia, molecular sieves, etc. [3–16]. At this juncture, it is noteworthy here that the product selectivity depends strongly on the nature and type of acidic sites present in these catalysts [5,12–19]. For example, weak or mild acidic catalysts like partially ion-exchanged (Na^+ or K^+) zeolite-Y [12] favor the formation of oxygen alkylated product, viz. *tertiary*-butyl phenyl ether (*t*-BPE), whereas a strong acidic catalyst, *e.g.*, zeolite-β [19], produces *meta-tertiary*-butyl phenol (*m-t*-BP). On the other hand, moderate acidic catalysts such as SAPO-11 [5], AlMCM-41 [14], FeMCM-41 [15] and zeolite-Y [12,13] lead to *p-t*-BP. Although the microporous catalysts such as SAPO-11 [5] and zeolite-Y [13] show good activity, the former, however, shows considerable amounts of cracked products and the latter produces 2,4-di-*tert*-butyl phenol (2,4-di-*t*-BP) [13]. On the other hand, the introduction of gallium into silicate or aluminosilicate molecular sieves has shown promise as catalysts for certain industrial processes, *i.e.*, transformation of C_3–C_5 alkanes into aromatics, hydrogen-transfer reactions, etc. [20,21]. Among the various solid acid catalysts, the one based on mesoporous metallosilicates [21,22] is promising, as the substitution of trivalent ions in the silicate framework leads to moderate acidity [14,15,20]. Realizing the importance of *p-t*-BP as well as the natural curiosity to check the catalytic activity of GaMCM-41, in the present investigation, an attempt was made to synthesize and characterize material as well as to study the catalytic properties of GaMCM-41 for the titled reaction.

2. Experimental section

2.1. Starting materials

Gallium nitrate nanohydrate ($Ga(NO_3)_3 \cdot 9H_2O$; Aldrich; 99.9%), fumed silica (SiO_2; Aldrich; 99.8%) and cetyltrimethylammonium bromide (CTAB, Aldrich; 99%) were used as sources for gallium, silicon and template, respectively. Tetramethylammonium hydroxide (TMAOH, Aldrich; 25 wt%) and sodium hydroxide (NaOH; Loba; 98%) were used as organic base and alkali sources. Phenol (Merck; 99.5%) and *tertiary*-butyl alcohol (*t*-BA; Thomas Baker; 99%) were used for (vapor-phase) phenol alkylation reactions. Authentic

* To whom correspondence should be addressed.

† This paper was presented at the International Symposium on Acid-Base Catalysis (IV) held at Matsuyama during 7–12 May 2001, O-18.

E-mail: selvam@iitb.ac.in

1011-372X/02/1100-0037/0

samples of *ortho-tertiary*-butyl phenol (*o-t*-BP; Fluka; 99%), *meta-tertiary*-butyl phenol (*m-t*-BP; Aldrich; 99%), *para-tertiary*-butyl phenol (*p-t*-BP; Fluka; 99%) and 2,4-di-*tertiary*-butyl phenol (2,4-di-*t*-BP; Fluka; 99%) were used for comparative analysis of the reaction products.

2.2. Synthesis of Na-GaMCM-41

Na-GaMCM-41 with a Si:Ga (molar) ratio of 30:90 was synthesized as per the literature procedure [21] with a typical molar gel composition of: 1 SiO_2:0.2 NaOH:0.27 TMAOH:0.27 CTAB:60 H_2O:xGa_2O_3 (where $x = 0.0055 - 0.0166$). First, TMAOH was dissolved in water. To this SiO_2 was added slowly, followed by NaOH. The mixture was stirred for 30 min. Another solution was prepared by mixing CTAB in distilled water and stirred for 30 min. Finally, both these solutions were mixed and stirred until a homogenous mixture was formed. Gallium nitrate was then added to this clear solution and was stirred for 1 h. The pH of the resulting gel was adjusted to 11.0 with dilute sulfuric acid and was aged for 16 h. The gel was transferred into Teflon-lined stainless steel autoclaves and kept in an air oven for crystallization at 423 K for three days. The solid product obtained was washed repeatedly, filtered and dried at 353 K for 12 h. The as-synthesized sodium form of the material (Na-GaMCM-41) was calcined at 823 K for 2 h in N_2, followed by air for 6 h.

2.3. Preparation of H-GaMCM-41

The protonated form of the mesoporous gallosilicate (H-GaMCM-41) was prepared from the calcined Na-GaMCM-41 by an ion-exchange method outlined previously [14,15]. Accordingly, NH_4-GaMCM-41 was first obtained by repeated exchange of Na-GaMCM-41 with 1M NH_4NO_3 at 353 K for 6 h. The H-GaMCM-41 was then obtained by deammoniation at 823 K for 6 h in air.

2.4. Characterization

All the samples were systematically characterized by powder X-ray diffraction (XRD; Rigaku), simultaneous thermogravimetry-differential thermal analysis (TG-DTA; Shimadzu), surface area analysis (sorptomatic-1990), Fourier transform infrared (FT-IR; Nicolet Impact 400) and inductively coupled plasma-atomic-emission spectroscopy (ICP-AES; Labtam Plasma 8440) techniques.

2.5. NH_3-TPD

The acidic behavior of the H-GaMCM-41 catalyst was studied by temperature-programmed desorption of ammonia (NH_3-TPD) as per the procedure described elsewhere [14]. About 200 mg of the protonated GaMCM-41 sample was placed in a quartz reactor and was activated at 773 K in air for 6 h, followed by 2 h in helium with a flow rate of 50 ml min^{1}. The sample was maintained at 373 K for 4 h prior to its exposure to 15 pulses of ammonia vapor (500 μl each), followed by purging with helium for 1 h. The desorption of ammonia was carried out by heating the reactor up to 873 K at a uniform rate of 10 K min^{-1} using a temperature programmer (Eurotherm). The amount of ammonia desorbed was estimated with the aid of a thermal conducting detector (TCD) signal as a response factor for ammonia. The desorption peaks were deconvoluted by using a Gaussian function with temperature as variant.

2.6. Tertiary butylation reaction

The tertiary butylation of phenol was carried out using 750 mg of H-GaMCM-41 catalyst in a homemade fixed-bed flow reactor. Prior to the reaction, the catalyst was activated at 773 K in flowing air for 8 h, followed by cooling to reaction temperature (448 K) under a nitrogen atmosphere. After 1 h, the reactant mixture, *i.e.*, phenol and *t*-butyl alcohol (*t*-BA) with a desired (molar) ratio and weight hour space velocity (WHSV), was fed into the reactor using a liquid injection pump (Sigmamotor) with nitrogen as carrier gas. The gaseous products obtained were cooled and the condensed liquid products were collected at 30 min intervals.

2.7. Product analyses

The various products of the tertiary butylation reaction, viz. *p-t*-BP, *o-t*-BP and *2,4*-di-*t*-BP, were identified by gas chromatography (NUCON 5700) with an SE-30 column. Further, *m-t*-BP was identified using an AT1000 column. In addition, all these products were confirmed with the use of a combined gas chromatography-mass spectrometry (GC-MS; HEWLETT G1800A) set-up fitted with an HP-5 capillary column.

3. Results and discussion

Figure 1 depicts the XRD patterns of GaMCM-41 in the as-synthesized, calcined and protonated forms, as well as after reaction. The diffraction patterns show all the major reflections, *i.e.*, 100, 110, 200, 210 and 300, which are typical characteristics of hexagonal mesoporous MCM-41 structures [22,23]. Table 1 summarizes the average unit cell parameters (a_0) and ICP-AES results for the various samples. It can be seen from table 1 that the gallium content remains nearly close to the starting (gel) composition, indicating the incorporation of gallium in the matrix. It is also interesting to note that the hexagonal unit cell parameter decreases with an increase in gallium content, which is in good agreement with Cheng *et al.*

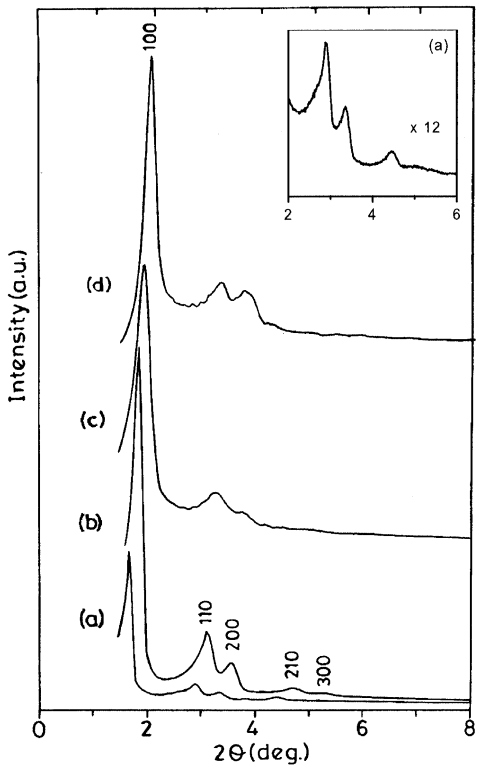

Figure 1. XRD patterns of various GaMCM-41(90). (a) As-synthesized Na-form, (b) calcined Na-form, (c) H-form (before reaction) and (d) H-form (after reaction).

[21] and Okumura *et al.* [24]. This observation is in contrast with the findings of aluminosilicate and ferrisilicate analogs where the insertion of larger cations, viz. Al^{3+} (0.53 Å) and Fe^{3+} (0.63 Å), for smaller Si^{4+} (0.40 Å) in the silicate framework invariably results in an expansion in the unit cell [14,15] because of longer M–O bonds, then Si–O bonds (Si–O = 1.62 Å; Al–O = 1.75 Å; Fe–O = 1.83 Å; Ga–O = 1.83 Å) [21]. The reasons for this discrepancy are not clear yet; however, the unexpected decrease in unit cell parameter for the gallosilicates, with larger Ga^{3+} (0.61 Å), could be attributed to poor condensation of gallosilicate polyanions vis-à-vis a decrease in wall thickness of the matrix [20,21].

TG of as-synthesized and calcined samples shows around 42% and 17% weight loss, respectively. BET surface area (650 $m^2 g^{-1}$) of calcined Na-GaMCM-41(60) is in good agreement with the reported values [20,21]. FT-IR spectra of calcined samples (figure 2)

Table 1
XRD and ICP-AES data of Na-GaMCM-41.

Samples [a]	a_0 (Å)		Si : Ga (molar ratio)	
	As-synthesized	Calcined	Synthesis gel	Calcined
Na-GaMCM-41(30)	53.92	53.64	30	25
Na-GaMCM-41(60)	57.75	55.47	60	54
Na-GaMCM-41(90)	59.96	55.82	90	81

[a] Number in parentheses indicates the nominal Si : Ga (molar) ratio.

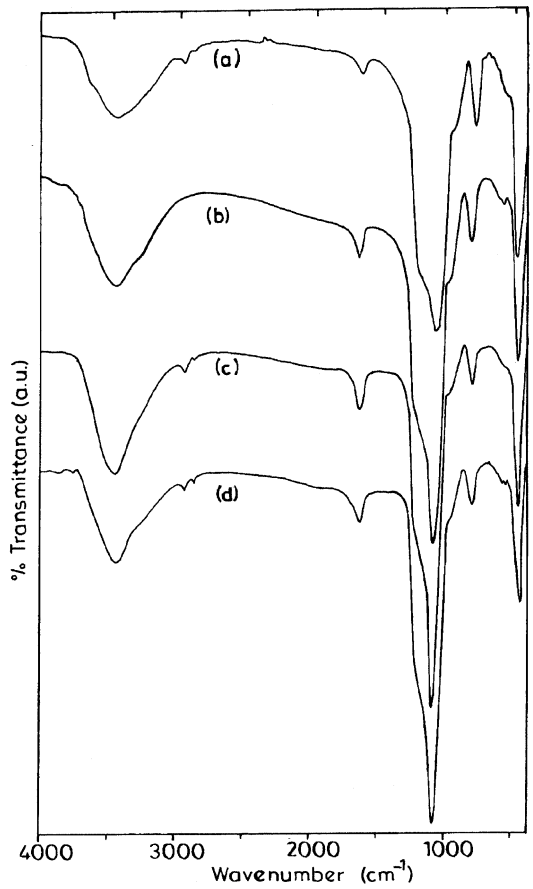

Figure 2. FT-IR spectra of calcined Na-GaMCM-41 with (a) Si/Ga = ∝, (b) Si/Ga = 90, (c) Si/Ga = 60 and (d) Si/Ga = 30.

show two main absorption bands around 1090 and 810 cm^{-1} respectively, corresponding to antisymmetric stretching and symmetric stretching vibration of ≡Si–O–T≡. The other absorption band around 465 cm^{-1} corresponds to a bending vibration of the ≡T–O– bond (T = Si or Ga). All these features are typical characteristics of the MCM-41 structure [20,25]. Furthermore, an increase in gallium content in the matrix causes a shift in the absorption bands toward lower wavenumbers from 466 cm^{-1} (Si/Ga = 90) to 462 cm^{-1} (Si/Ga = 30). For the corresponding silicates (Si/Ga = ∝) a further shift toward higher wavenumber (468 cm^{-1}) is noticed. The progressive shift could be attributed to an increase in mean T–O distances (Si–O = 1.62 Å; Ga–O = 1.83 Å) [20].

Figure 3 shows NH_3-TPD patterns of various H-GaMCM-41. The observation of a broad distribution of acidic sites is in good agreement with Okumura *et al.* [24]. The peaks were deconvolved using a Gaussian function [26] with temperature as the variant, which resulted in five different types of acid sites, viz. (i) weak (or) mild Brönsted, (ii) moderate Brönsted, (iii) strong Brönsted, (iv) weak Lewis and (v) strong Lewis [14,15,20,24]. They are assigned as follows: the weak acid or type (i) sites arise from surface hydroxyl groups,

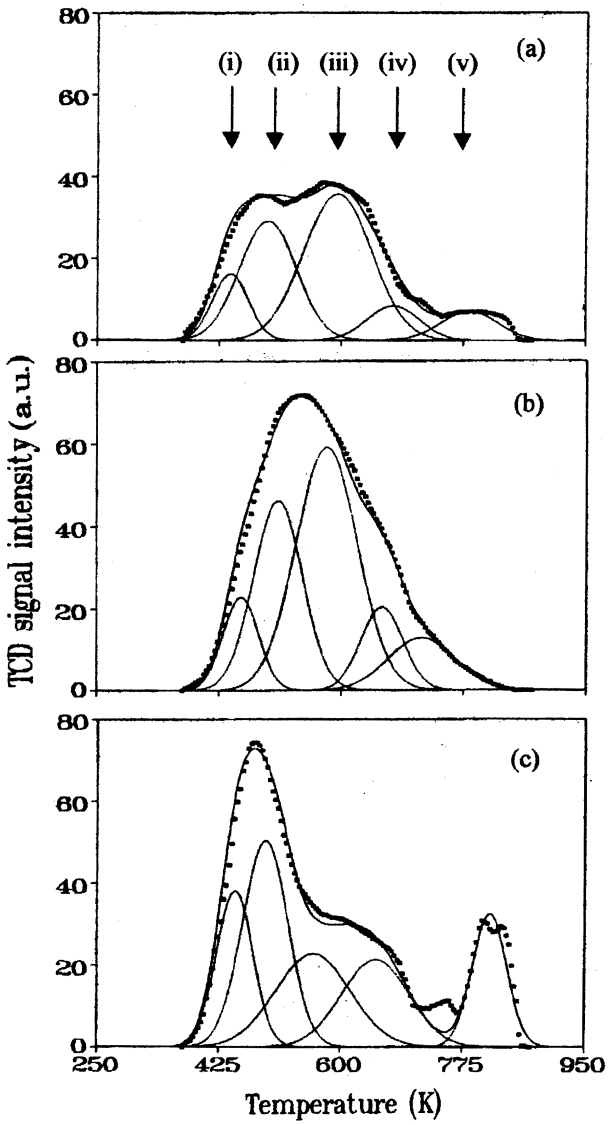

Figure 3. NH_3-TPD profiles of H-GaMCM-41 with (a) Si/Ga = 90, (b) Si/Ga = 60 and (c) Si/Ga = 30.

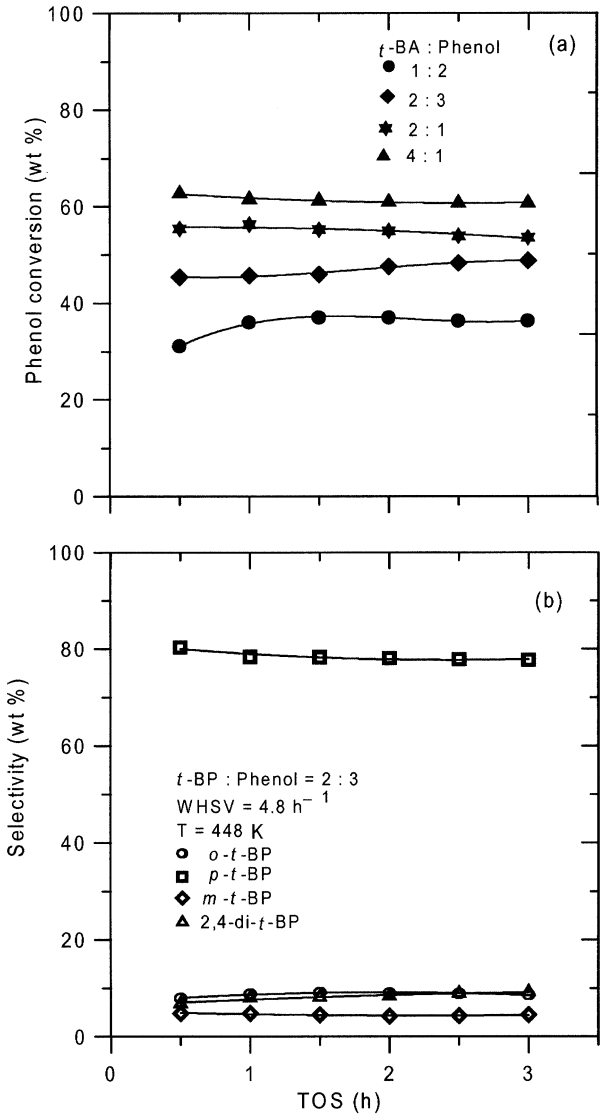

Figure 4. Effect of time-on-stream over H-GaMCm-41(60): (a) phenol conversion and (b) product selectivity.

whereas the moderate or type (ii) and strong or type (iii) sites originate from structural (Brönsted) acid sites as a result of the presence of trivalent gallium in the silicate (matrix) [15,24]. On the other hand, the type (iv) peak may result from structural Lewis acid sites. However, the broad peak at higher temperature is due to strong Lewis acid sites, which may arise from octahedral gallium. It is, however, clear from the figure that the area under the profiles corresponding to the moderate and strong Brönsted acid sites is much larger (~50–70%), which may primarily be useful for the chosen reaction [26]. It can also be seen from figure 3 that the total amount of acid sites increase with an increase in gallium content. Furthermore, the relative area of type (ii) and type (iii) acid sites increases with an increase in gallium. However, for Si : Ga = 30 a significant decrease in the type (iii) acid site is noticed. This observation could be attributed to the presence of type (iv) and type (v) sites as a consequence of the formation of octahedral gallium ions.

Figure 4(a) shows the effect of time-on-stream (TOS) on phenol conversion over H-GaMCM-41(60). It is clear from the figure that the catalyst does not show any deactivation at higher phenol (or lower *t*-BA) content. However, a slight deactivation is noted at lower phenol (or higher *t*-BA) content due to dehydration and/or polymerization of *t*-BA leading to coke formation [4,14–16]. Therefore, for the further studies, an optimum molar fed mixture (phenol : *t*-butyl alcohol) of 3 : 2 molar ratios was chosen. Figure 4(b) depicts the effect of TOS on product selectivity. It can be seen from the figure that *p*-*t*-BP slightly decreases after 1.5 h while the corresponding 2,4-di-*t*-BP selectivity increases. However, there is no appreciable change in the selectivity of *o*-*t*-BP and *m*-*t*-BP.

Figure 5 depicts the effect of temperature on the reaction over H-GaMCM-41(60). It can be seen from the figure that the phenol conversion decreases as the reaction temperature increases, which could be attributed

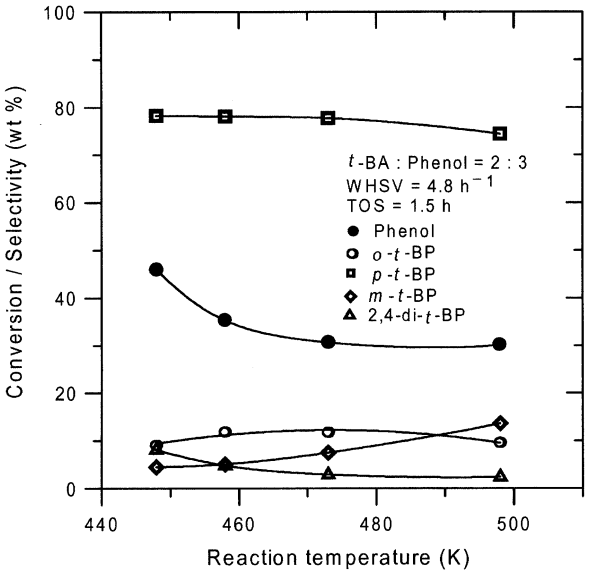

Figure 5. Effect of reaction temperature over H-GaMCM-41(60) for the tertiary butylation of phenol reaction.

to a simultaneous dealkylation of the *t*-BP leading to phenol [5,13,14]. Furthermore, at higher temperature, 2,4-di-*t*-BP selectivity decreases owing to the absence of secondary alkylation, which again supports the dealkylation process at higher temperature. Hence, an increase in selectivities of both *o*-*t*-BP and *p*-*t*-BP is expected. On the contrary, a slight decrease in selectivity is noticed with temperature. This observation, however, could be accounted for by a possible rearrangement of *o*- and *p*-products into thermodynamically favorable *m*-*t*-BP [14,16,17]. Figure 6 shows the effect of WHSV on reaction over H-GaMCM-41(60). It is clear from the figure that with the increase in WHSV, the substrate conversion initially increases and then decreases smoothly. The observed lower conversion at low WHSV could possibly be due to dealkylation of *t*-BP owing to a longer contact time of products with the catalyst [14–17]. However, at higher WHSV the lower conversion could be attributed to fast diffusion of the reactant molecules, and the increase in mono-alkylated products could be due to the absence of a secondary reaction as a consequence of less contact time of reactants/products with the catalyst.

Figure 7 shows the effect of *t*-BA-to-phenol ratio on the reaction over H-GaMCM-41 with different Si/Ga

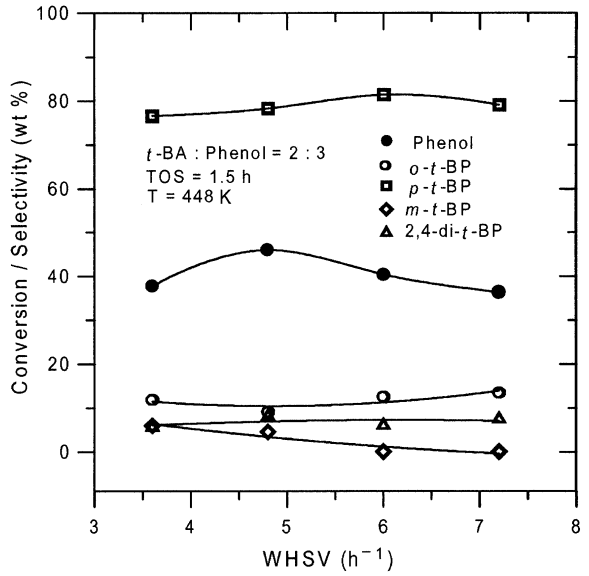

Figure 6. Effect of space velocity over H-GaMCM-41(60) for the tertiary butylation of phenol reaction.

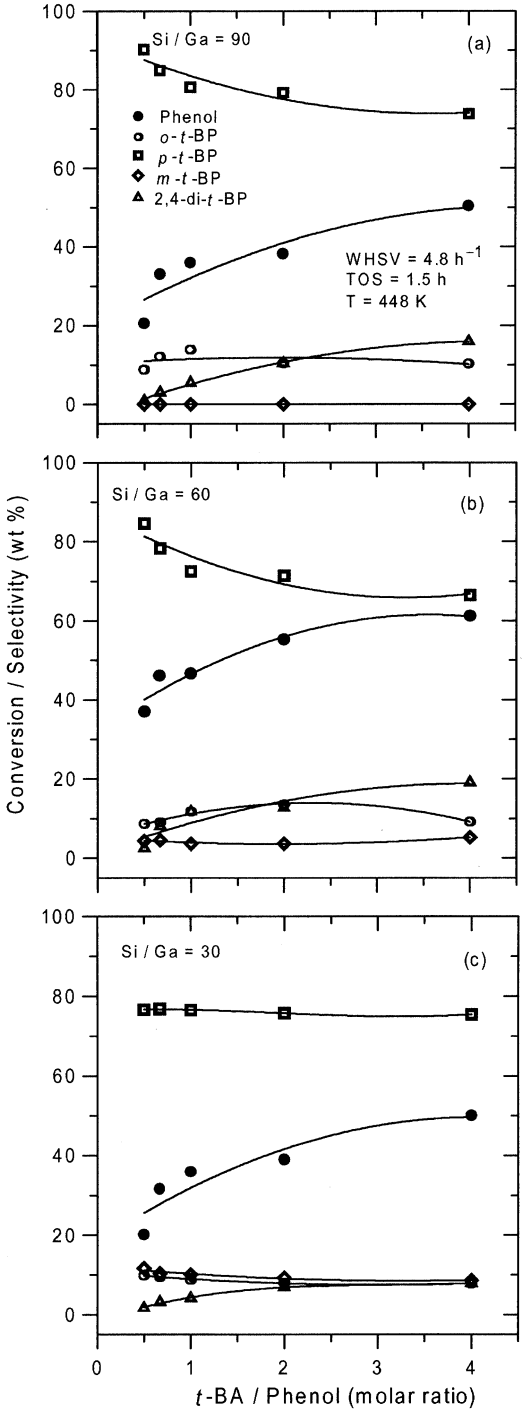

Figure 7. Effect of *t*-BA/phenol molar ratio over H-GaMCM-41 with (a) Si/Ga = 90, (b) Si/Ga = 60 and (c) Si/Ga = 30.

Table 2
Effect of Si : Ga ratio on the reaction. [a]

Reactant/products	H-GaMCM-41 (30)	H-GaMCM-41 (60)	H-GaMCM-41 (90)
Phenol conversion (wt%)	20.2	37.0	20.5
Selectivity (%)			
o-*t*-BP	9.9	8.7	8.8
m-*t*-BP	11.7	4.3	–
p-*t*-BP	76.7	84.6	90.2
2,4-di-*t*-BP	1.7	2.4	1.0

[a] Reaction conditions: $T = 448$ K; WHSV $= 4.8\ h^{-1}$; TOS $= 1.5$ h; *t*-BA : phenol $= 1:2$.

ratios. It can be seen from the figure that in all cases, phenol conversion increases with an increase in *t*-BA, owing to a competitive adsorption between *t*-BA over phenol [14,18]. Furthermore, *p*-*t*-BP is obtained as a major product along with small amounts of *o*-*t*-BP, *m*-*t*-BP and 2,4-di-*t*-BP. However, an increase in *t*-BA content leads to a decrease in *p*-*t*-BP selectivity due to a possible secondary alkylation reaction. This is well supported by the observed increase in 2,4-di-*t*-BP. It can also be seen from figure 7(a) that an increase in 2,4-di-*t*-BP is noticed for the low gallium-containing samples, while it is low for the high gallium sample (figure 7(c)). The low selectivity of 2,4-di-*t*-BP of the latter could be attributed to the presence of relatively small amounts of type (iii) acid sites (*cf.* figure 3). Furthermore, the formation of *m*-*t*-BP was also noted for the high gallium-containing sample owing to the presence of relatively more type (iv) acid sites.

Table 2 summarizes the resulting phenol reaction over H-GaMCM-41 with different Si : Ga ratios under optimized experimental conditions. It can be seen from the table that the phenol conversion increases with an increase in gallium content, *i.e.*, from (Si : Ga ratio) 90 to 60. The observed increase in conversion could be attributed to an increase in moderate and strong (type (ii) and type (iii)) acid sites (see figure 3). The results are in good agreement with our earlier results on mesoporous H-AlMCM-41 and H-FeMCM-41. However, at further increase in gallium content, *i.e.*, Si : Ga = 30, both the (phenol) conversion and (*p*-*t*-BP) selectivity decreases possibly due to the following reasons: (a) dealkylation of *p*-*t*-BP; (b) isomerization of *p*-*t*-BP into *m*-*t*-BP owing to the presence of type (iv) acid sites, which normally favor the isomerization reactions [13]. Table 3 presents a comparison of the results of tertiary butylation of phenol over various mesoporous metallosilicate molecular sieves. Although *p*-*t*-BP selectivity over these catalysts remains nearly the same, the phenol conversion is slightly higher in the case of gallosilicates. The higher conversion can, however, be explained on the basis of the nature of acid sites present in these catalysts (figure 8). As can be seen from the figure, the area under the type (ii) and type (iii) acid sites for H-GaMCM-41, H-AlMCM-41 and H-FeMCM-41 is 70%, 62% and 56%, respectively. Thus, the presence of higher moderate-to-strong acid sites, *i.e.*, type (ii) and type (iii), in H-GaMCM-41 may clearly be responsible for the observed higher phenol conversion.

4. Conclusions

In summary, it can be deduced from this study that mesoporous H-GaMCM-41 is a promising catalyst for the *para*-selective *t*-butylation of phenol reaction. The increase in gallium content increases in conversion. However, a further increase in gallium (Si : Ga = 30) leads to dealkylation and a secondary isomerization reaction, which thus decreases both conversion and selectivity owing to the formation of octahedral gallium species. Furthermore, the gallosilicates possess relatively high moderate-to-strong (Brönsted) acid sites over the

Table 3
Effect of various trivalent cations on the reaction. [a]

Reactant/products	H-GaMCM-41 (this work)	H-AlMCM-41 (14)	H-FeMCM-41 (15)
Phenol conversion (wt%)	37.0	31.0	8.4
Selectivity (%)			
o-*t*-BP	8.7	8.1	16.2
m-*t*-BP	4.3	6.4	–
p-*t*-BP	84.6	84.2	83.8
2,4-di-*t*-BP	2.4	1.3	–

[a] Reaction conditions: $T = 448$ K; WHSV $= 4.8\ h^{-1}$; TOS $= 1.5$ h; *t*-BA : phenol $= 1:2$.

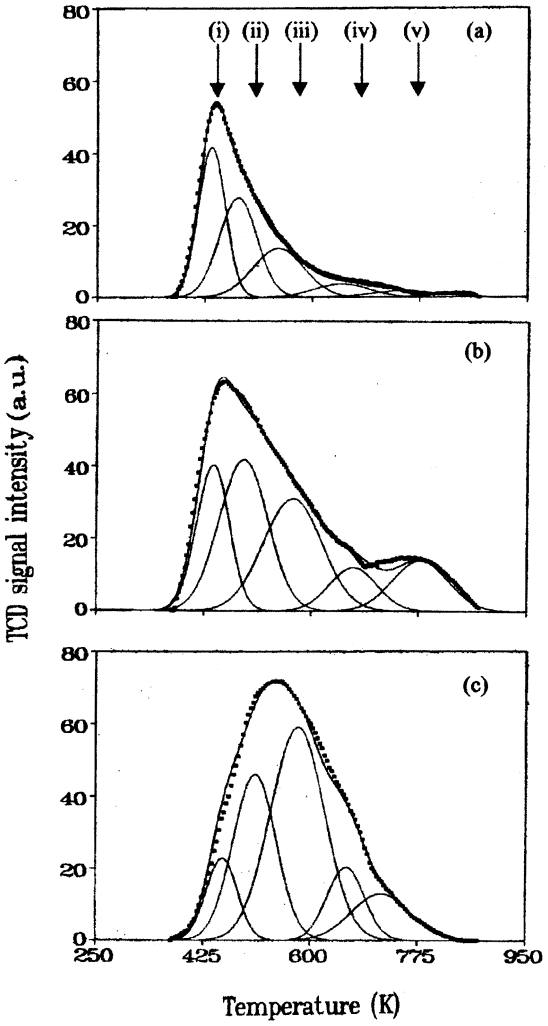

Figure 8. NH_3-TPD profiles of (a) H-FeMCM-41, (b) H-AlMCM-41 and (c) H-GaMCM-41.

corresponding aluminosilicates and ferrisilicates, which clearly accounts for the different activities of these catalysts for the chosen reaction.

Acknowledgment

The authors thank RSIC, IIT-Bombay for ICP-AES and GC-MS facilities.

References

[1] S.H. Patinuin and B.S. Friedman, in: *Alkylation of Aromatics with Alkenes and Alkanes in Friedel Crafts and Related Reactions*, Vol. 3, ed. G.A. Olah (Interscience, New York, 1964) p. 75.
[2] J.F. Lorenc, G. Lambeth and W. Scheffer, in: *Kirk-Othmer Encyclopedia of Chemical Technology*, Vol. 2, ed. M. Howe-Grant and J.I. Kroschwitz (Wiley and Sons, New York, 1992) p. 113.
[3] K.G. Chandra and M.M. Sharma, Catal. Lett. 19 (1992) 309.
[4] A.J. Kolka, J.P. Napolitano and G.G. Elike, J. Org. Chem. 21 (1956) 712.
[5] S. Subramanian, A. Mitra, C.V.V. Satyanarayana and D.K. Chakrabarty, Appl. Catal. A 159 (1997) 229.
[6] K. Kanekichi and T. Yasuo, Japanese Patent (1975) 75 112 325.
[7] C.D. Chang and S.D. Hellring, U.S. Patent (1994) 5 288 927.
[8] M. Yamamoto and A. Akyama, Japanese Patent (1994) 6 122 639.
[9] A.U.B. Queiroz and L.T. Aikawa, French Patent (1994) 2 694 000.
[10] E.M. Viorica, E.S.A. Meroiu, H. Justin, O. Maria and C. Eleonora, Rom. Patent (1981) 73 994.
[11] R.A. Rajadhyakasha and D.D. Chaudhari, Ind. Eng. Chem. Res. 26 (1987) 1276.
[12] A. Corma, H. Garcia and J. Primo, J. Chem. Res. (s) (1988) 40.
[13] K. Zhang, C. Hunag, H. Zhang, S. Xiang, S. Liu, D. Xu and H. Li, Appl. Catal. A 166 (1998) 89; K. Zhang, H. Zhang, G. Xu, S. Xiang, D. Xu, S. Liu and H. Li, Appl. Catal. A 207 (2001) 183.
[14] A. Sakthivel, S.K. Badamali and P. Selvam, Micropor. Mesopor. Mater. 39 (2000) 457.
[15] S.K. Badamali, A. Sakthivel and P. Selvam, Catal. Lett. 65 (2000) 153.
[16] A. Sakthivel, N. Saritha and P. Selvam, Catal. Lett. 72 (2001) 225.
[17] S. Namba, T. Yahima, Y. Itaba and N. Hara, Stud. Surf. Sci. Catal. 5 (1980) 105.
[18] R.F. Parton, J.M. Jacobs, D.R. Huybrechts and P.A. Jacops, Stud. Surf. Sci. Catal. 46 (1988) 163.
[19] A. Mitra, Ph.D Thesis, IIT-Bombay, 1997.
[20] H. Kosslick, H. Landmesser and R. Fricke, J. Chem. Soc. Faraday Trans. 93 (1997) 1849; R. Fricke, H. Kosslick, G. Lischke and M. Richter, Chem. Rev. 100 (2000) 2303.
[21] C.F. Cheng, H. He, W. Zhou, J. Klinowski, J.A.S. Goncalves and L.F. Gladden, J. Phys. Chem. 100 (1996) 390; C.F. Cheng, M.D. Alba and J. Klinowski, Chem. Phys. Lett. 250 (1996) 328.
[22] J.S. Beck, J.C. Vartuli, W.J. Roth, M.E. Leonowicz, C.T. Kresge, K.D. Schmitt, C.T.-W. Chu, D.H. Olson, E.W. Sheppard, S.B. McCullen, J.B. Higgins and J.L. Schlenker, J. Am. Chem. Soc. 114 (1992) 10834.
[23] P. Selvam, S.K. Bhatia and C. Sonwane, Ind. Eng. Chem. Res. 40 (2001) 3237.
[24] K. Okumura, K. Nishigaki and M. Niwa, Chem. Lett. (1998) 577; Micropor. Mesopor. Mater. 44–45 (2001) 509.
[25] K. Vidya, S.E. Dapurkar, P. Selvam, S.K. Badamali, D. Kumar and N.M. Gupta, J. Mol. Catal. A 181 (2002) 91.
[26] S.K. Badamali, A. Sakthivel and P. Selvam, in: *Adsorption Science and Technology*, ed. D.D. Do (World Scientific, Singapore, 2000) p. 553.